Ultraviolet vs. visible skylight polarization measurements

Antoine Moutenet, Julien Serres, Stéphane Viollet

Ultraviolet vs. Visible Skylight Polarization Measurements

Antoine Moutenet[1,2], Julien R Serres[1,3], Stephane Viollet[1]

[1] : Aix Marseille Univ, CNRS, ISM [2] :Safran Electronics&Defense [3]: Institut Universitaire de France

JJCR2023

Insects using skylight polarization for autonomous outdoor navigation

Autonomous outdoor navigation is mainly based on Global Navigation Satellite Systems (GNSS), magnetic compass and gyro-compass but it requires redundant, robust and affordable strategies to be reliable in all conditions (wheather, electromagnetic disturbances...). Inspired by bees and some ants which are known to use skylight linear polarization for their outside moving heading calculation, a lot of bio-inspired compass using visible skylight polarization were made **[1]**.

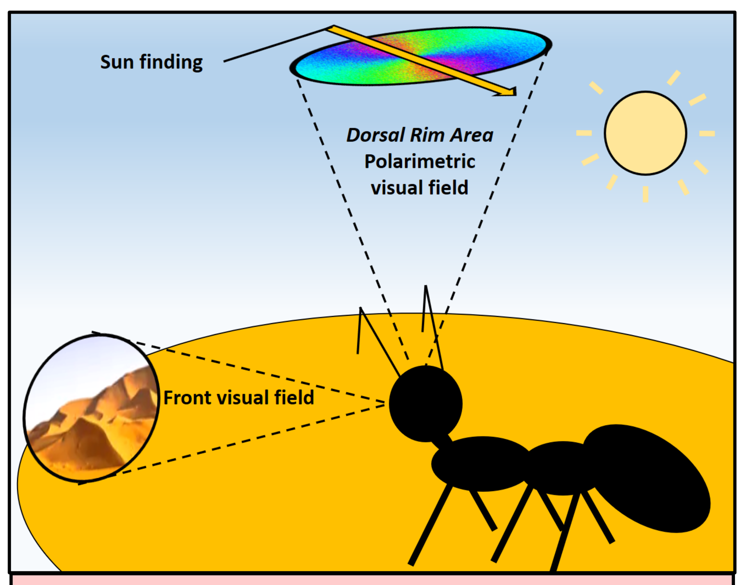

Fig. 1. Schematic use of the different fields of view of the Sahara's cataglyphis for navigation

Those sensors, basically sun-finder devices,. coupled with ephemerides computation in order to find true North, provides good results but are still unreliable in highly overcast sky conditions.

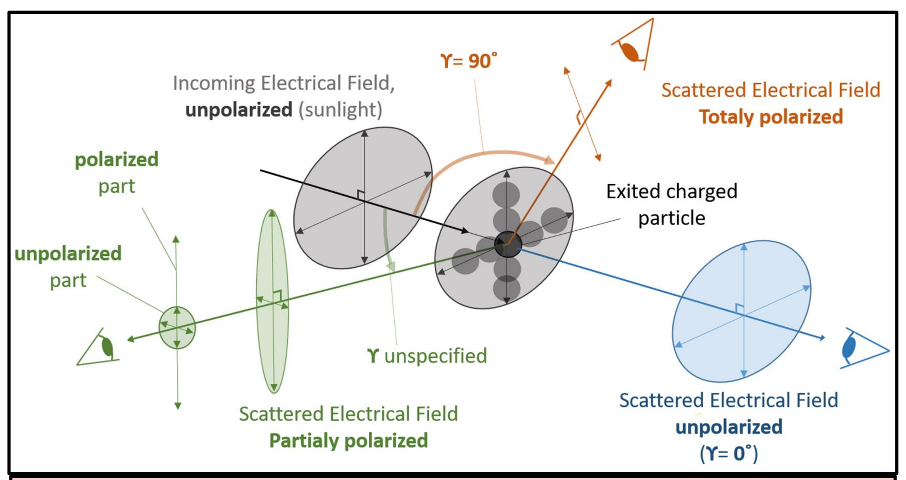

Fig. 2. Skylight single scattering and polarization. The polarization depends on the relative positions of illuminant, scattering particle and observer. γ is the scattering angle.

If the UV are not supposed to be reliable under clear sky, insects are curiously also sensitive to linear polarization in this spectral band **[2]**.

We chose, as some of our peers [3]–[7], to compare UV and visible skylight polarization measurements in order to understand if UV could be used to improve heading estimation under overcast skies.

Skylight polarization measurement and polarization formalism

The single scattering model is reliable only for near visible spectrum in clear sky conditions. In facts clouds and aerosols lead to changes in the AoP distribution and in the count of points featuring null DoLP, from 2 to 4 **[8],[9]**. Only two polarization parameters remains :

- the symmetry around solar meridian axis
- the existence of a segment verifying AoP_L=90˚ on the solar meridian axis

We computed DoLP and AoP_L in **Fig. 5**, using the normalized Stokes parameters s_1 and s_2 as follows, with α_p the azimuth coordinate of each pixel in the image frame:

$$s_1 = (I_0 - I_{90})/(I_0 + I_{90})$$
$$s_2 = (I_{45} - I_{135})/(I_{45} + I_{135})$$
$$DoLP.e^{2i.AoP_L} = (s_1 + i.s_2).e^{-2i.\alpha_P}$$

We use on both images taken by the UV and polarimetric cameras the same image processing algorithms :

- one which displays AoP_L and DoLP
- one sun azimuth axis finder, relying on a binary threshold of ±90◦ AoP_L points and Hough transform **[10].**

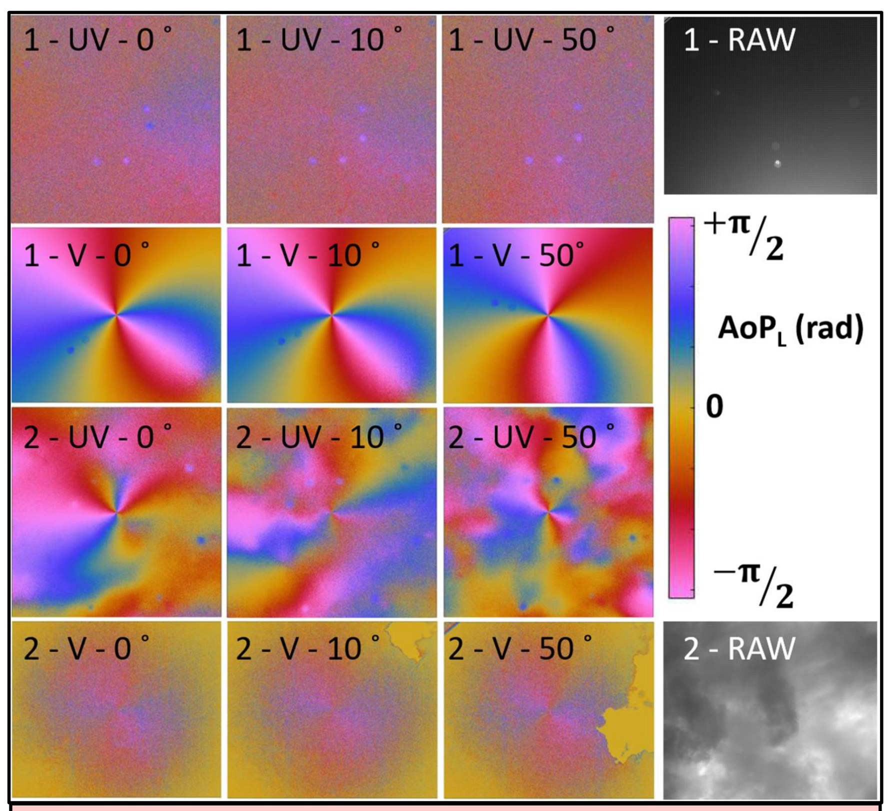

Fig. 5. Examples of AoPl patterns computed from real images. 1 & 2 refer to two sky conditions, clear & thick cloud blanket respectively. UV is for AoPl in the UV, V for AoPl in the visible spectrum. 0◦, 10◦, 50◦ correspond to the angular position of the support rail. RAW is a monochromatic image of the sky.

Conclusion and futur work

As expected from studies carried out on insects, the use of a UV-sensitive camera enhanced with polarized light measurement ability has shown that it could be possible to estimate the sun azimuth under overcast skies.

Nevertheless, this study requires further experiments by mounting a genuine objective mounted on the UV-camera to decrease skydrift effects and achieve a fair comparison with snapshot polarimetric camera sensitive to the visible spectrum.

The first step will be to use a UV objective lenses will allow us to reduce drastically the acquisition time of the camera, due to aperture increasement. The second one will be to use four of these cameras mounted with static linear UV polarizer, one for each linear polarization that classic polarimetric camera are sensitive to.

Experimental Setup

Our experimental setup **(Fig. 3)** was composed of two camera set on one motorized rotating support rail :

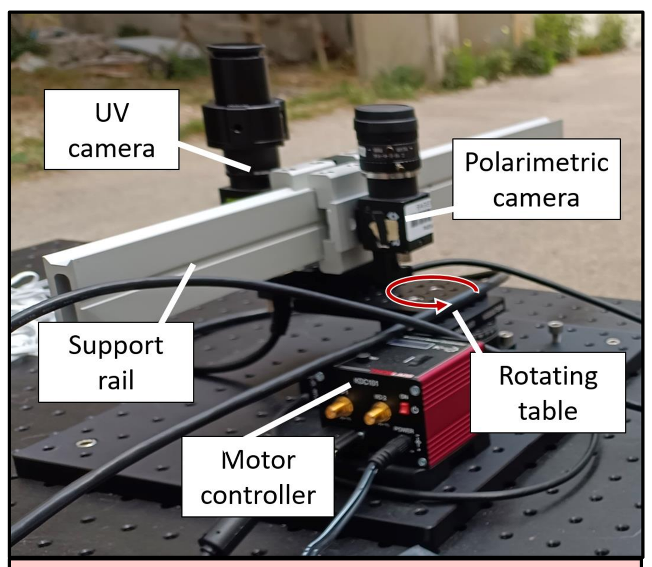

Fig. 3. Outdoor experiment setup. Luminy University Campus, Marseille.

– a polarized monochromatic camera (26◦ half field of view). It is made of a CMOS sensor with an add-on micro-polarizers array such as, for each square block of four pixels, the four micro-polarizers orientations are at 0, 45, 90 and 135◦ from the sensor length, see **Fig. 4(a)**.
Its acquisition time is less than 0.1s

– a UV-sensitive camera (15◦ half field of view). With, as an objective, a pinhole (50µm or 200µm) and a UV-centered band-pass filter, see **Fig. 4(b)**. Above this elementary UV objective was connected a manually continuous rotating mount (1◦ precision) with a UV polarizer inside, in order to be able to take images of linear polarization orientations at 0, 45, 90 and 135◦ from the sensor length, and to merge those image into polarimetric camera-like image. Its acquisition time was 8s for the 50µm pinhole and 2s for the 200µm pinhole. The time interval between each images was between 3 and 5s.

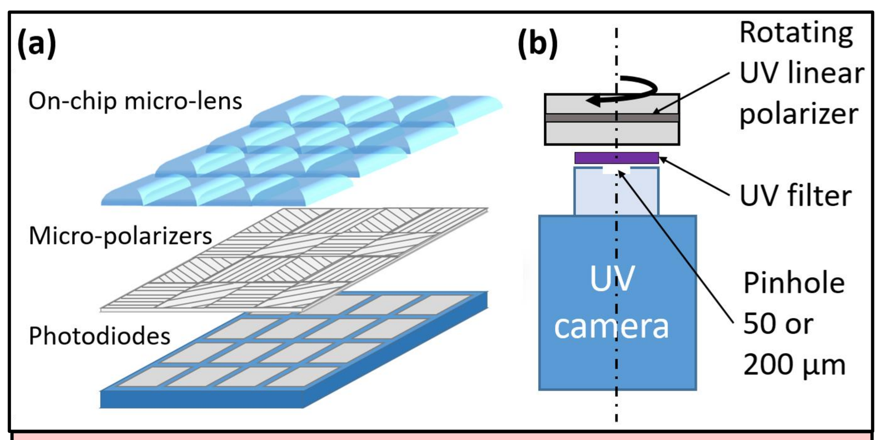

Fig. 4. (a) Visible spectrum polarized camera **(b)** UV-sensitive camera fitted with a low-cost objective.

Measurements were made at Marseille in France, June 2023. For each measurement, we oriented the SR according to three positions: 0, 10 and 50 ◦ from the rotating table origine.

Measurements results

sky	measured sun azimuth axis (°) SR at 0 deg	SR at 10 deg	SR at 50 deg	sky drift	azimuth step consistency
clear	32.07	37.2	79.19	low	✓
	35.17	44.2	82.48	-	✓
few clouds	43.15	-2.7	47.06	strong	✗
	63.36	71.81	-68.7	-	✓
clouds	37.93	35.52	22.7	low	✗
	38.2	45.07	48.86	-	✗
big clouds	78.71	-43.33	-37.42	strong	✗
	-89.46	-1.12	0.07	-	✗
thin cloud blanket	17.2	24.56	31.04	medium	✗
	32.76	40.57	79.91	-	✓
thin cloud blanket	16.92	18.15	16.04	null	✗
	32.91	34.22	48.31	-	✗
thick cloud blanket	-4.77	-6.31	41.18	strong	~
	47.32	51.04	42.47	-	✗

Table 1. Sun azimuth estimation examples for various skies. Each experiment under one sky condition is separated in 3 angular positions of the support rail. Shaded boxes are for UV and clear boxes for visible spectrum. Mesured azimuth's axis takes value between −90◦ and +90◦.
Sky drift refers to changes in skylight intensity while UV captures. Azimuth step consistency refers to correspondence between azimuth measurement and stage rotation steps.

Sky drift due to the long-time UV captures affected measurements. In order to estimate the sky drift's impact we captured, for each experiment 4 images with the UV camera, with a fixed polarizer position. Then, we merged them like the classical captures and use them to compute a fake DoLP. The fake DoLP value indicate the level of sky drift impact.
We classified the intensities of the sky drift as follows : null, low, medium, strong and very strong (**Fig. 6**).

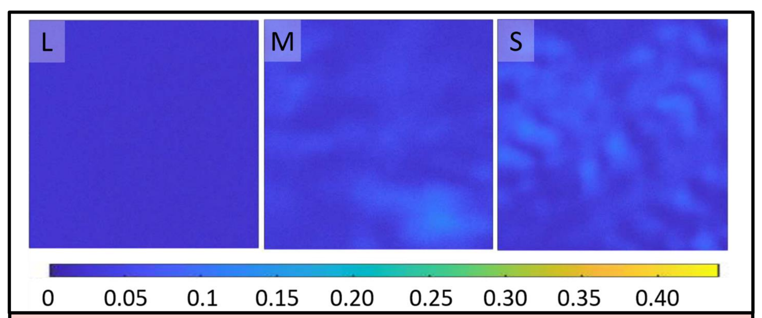

Fig. 6. Fake DoLP examples for sky drift level estimation. **L :** low sky drift, **M :** medium, **S :** strong sky drift.

Experiments' results are displayed in **Table 1. S**ince the sun is always moving, the steps expected in azimuth measurements are 9◦ and 39◦, instead of 10◦ and 40◦.

In **Table 1 t**he first double row (clear) corresponds to **measurement 1 in Fig. 5** and **L in Fig. 6**, seventh double row (thick cloud blanket) corresponds to measurement **2 in Fig. 4** and **S in Fig. 5**, and the fifth double row (thin cloud blanket) corresponds to M in **Fig. 5**.

[1] F. Kong, Y. Guo, J. Zhang, X. Fan, X. Guo, "Review on bio-inspired polarized skylight navigation," Chinese Journal of Aeronautics, May 2023.
[2] G. Horv´ath and D. Varj´u, "Polarized Light in Animal Vision," 2004.
[3] X. Wang, J. Gao and Z. Fan, "Empirical corroboration of an earlier theoretical resolution to the UV paradox of insect polarized skylight orientation,"Naturwissenschaften, 2014.
[4] I. Pomozi, G. Horv´ath, and R. Wehner, "How the clear-sky angle of polarization pattern continues underneath clouds : full-sky measurements and implications for animal orientation," Journal of Experimental Biology, 2001.
[5] M. Blumthaler and M. Schwarzmann, "Spectral measurements of the polarization of UV sky radiance," SPIE, 2005.
[6] N. Carey, and W. Sturzl, "An insect-inspired omnidirectional vision system including UV-sensitivity and polarisation," IEEE International Conference on Computer Vision Workshops, 2011.
[7] H. Zhao, W. Xu, "A Bionic Polarization Navigation Sensor and Its Calibration Method," Sensors , Vol. 16, No. 8, August 2016.
[8] M. V. Berry, M. R. Dennis, and R. L. Jr Lee, "Polarization singularities in the clear sky," New Journal of Physics, 2004.
[9] G. Horvath, B. Bernath, B. Suhai, and A. Barta, "First observation of the fourth neutral polarization point in the atmosphere," JOSA, 2002.
[10] H. Lu 1, Y. Xie, K. Zhang, H. Zhang, X. M. Zou, J. Wang, and K. C. Zhao, "Construction and test of bio-inspired imaging polarization navigation prototype," The International Archives of the Photogrammetry, Remote Sensing and Spatial Information Sciences, August 2020.

A.M. was supported by a CIFRE doctoral fellowship from the ANRT and Safran Electronics & Defense (agreement #2021/0056).
J.R.S has received funding from the Excellence Initiative of Aix-Marseille Université A*Midex, a French "Investissements d'Avenir" programme AMX-21-ERC-02 and AMX-20-TRA-043.
This research work was also supported by the SUD Provence-Alpes-Côte d'Azur Region (PACA) (Grant#2021/08135).